Thalamic network controllability changes and cognitive impairment in multiple sclerosis

Running title: Thalamic network controllability in MS

Yuping Yang[1], Anna Woollams[1], Ilona Lipp[2], Zhizheng Zhuo[3], Valentina Tomassini[4], Yaou Liu[3*], Nelson Trujillo-Barreto[1*], Nils Muhlert[1*]

[*]These authors contributed equally to this work as joint senior authors

[1]Division of Psychology, Communication and Human Neurosciences, Faculty of Biology, Medicine and Health, University of Manchester, Manchester, UK

[2]Department of Neurophysics, Max Planck Institute for Human Cognitive and Brain Sciences, Leipzig, Germany

[3]Department of Radiology, Beijing Tiantan Hospital, Beijing, China

[4]Institute for Advanced Biomedical Technologies (ITAB), Department of Neurosciences, G. d'Annunzio University of Chieti-Pescara, Chieti, Italy

Correspondence to: Dr Nils Muhlert

Division of Psychology, Communication and Human Neurosciences

Faculty of Biology, Medicine and Health

University of Manchester, Oxford Road, Manchester M13 9PL, UK

E-mail: nils.muhlert@manchester.ac.uk

Abstract:

Multiple sclerosis is a neuroinflammatory and neurodegenerative disease commonly associated with cognitive impairment. Understanding brain mechanisms of cognitive impairment in multiple sclerosis is crucial for early diagnosis and developing effective interventions to improve the quality of life in patients. Recent studies indicate that individuals with multiple sclerosis who develop cognitive impairment display changes in network activity in the brain, such as altered transitions between network states (network activity patterns). Particularly, regions within the subcortical network, like the thalamus, show abnormalities early in multiple sclerosis, possibly driving the subsequent changes in the rest of the brain. In this study, we investigated whether there are brain regions specifically involved in driving network changes throughout the brain in multiple sclerosis, and assessed how this relates to cognitive impairment in patients. To this end, we constructed functional brain networks based on resting-state functional MRI data from 102 multiple sclerosis patients and 27 healthy controls. Then we applied network controllability analysis using the most commonly used controllability measures to quantify the effect that brain networks or regions have on driving network changes and state transitions in multiple sclerosis. Furthermore, we compared network controllability changes between patients with different cognitive status. Finally, we tested the reproducibility of our main results using a separate dataset of 95 multiple sclerosis patients and 45 healthy controls. We found significant global, cortical, and subcortical controllability changes in multiple sclerosis, as indicated by increased average controllability while decreased modal controllability and decreased activation energy in patients compared to controls. These changes predominately concentrated in the subcortical network, particularly the thalamus, and were further confirmed in the replication dataset. The controllability changes suggest a compensatory strategy in the brain network of patients, towards preserving fundamental transitions between easy-to-reach network states while relinquishing energetically costly transitions between difficult-to-reach network states. Moreover, while both cognitively impaired and cognitively preserved patients showed controllability changes compared to healthy controls, the thalamus in cognitively impaired patients exhibited a significantly greater increase in average controllability than cognitively preserved patients. This emphasizes the crucial role of the thalamus in the emergence of cognitive impairment in multiple sclerosis. Overall, this study highlights the effect that the subcortical network and the thalamus has on driving network changes across the brain in multiple sclerosis and especially in those cognitively impaired

patients, suggesting a possible brain mechanism underpinning cognitive impairment in individuals with multiple sclerosis.

Keywords: Multiple sclerosis; cognitive impairment; thalamus; subcortical network; network controllability; resting-state fMRI

Abbreviations:

BRB-N = Brief Repeatable Battery of Neuropsychological Tests; CIMS = cognitively impaired multiple sclerosis; CPMS = cognitively preserved multiple sclerosis; DAN = dorsal attention network; DMN = default mode network; EDSS = Expanded Disability Status Scale; FA = flip angle; FLAIR = fluid-attenuated inversion recovery; FPN = frontoparietal network; HC = healthy control; LN = limbic network; MS = multiple sclerosis; MSFC = Multiple Sclerosis Functional Composite; PASAT3 = Paced Auditory Serial Addition Task 3 seconds; ROI = region of interest; rs-fMRI = resting-state functional MRI; SD = standard deviation; SMN = somatomotor network; VAN = ventral attention network; VN = visual network; 25-FWT = 25 Foot Walk Test; 3DT1 = 3D T1-weighted sequence; 9-HPT = 9 Hole Peg Test.

Introduction

Multiple sclerosis (MS) is a neuroinflammatory and neurodegenerative disease that mainly affects the central nervous system. Cognitive impairments are common in MS, with estimated prevalence ranging from 43% to 70%.[1] Cognitive dysfunction in MS encompasses deficits in attention, memory, information processing speed, verbal memory and fluency, executive function, and visuospatial function, which can have a significant impact on daily activities of people with this disease.[2] Understanding the brain mechanisms of cognitive dysfunction in MS is crucial for developing effective interventions and improving the life quality of patients.

Recent studies for cognitive impairments in MS suggest they arise due to changes within core activity networks within the brain. For example, a number of studies report altered connectivity in the default mode network (DMN), which are associated with deficits in memory, attention and verbal fluency in people with MS.[3–6] A useful recent model suggests that MS patients with cognitive impairment (CIMS) switch less between brain states (network activity patterns) compared to cognitively preserved patients (CPMS),[7,8] and exhibit reduced functional connectivity between the subcortical network and DMN in specific states.[8] The subcortical regions, which are strongly connected to the rest of the brain, have gained wide attention in MS, with many studies reporting associations between cognitive impairment and functional connectivity changes in the subcortical network[8–10] as well as in specific regions within the subcortex, such as the thalamus,[11–14] hippocampus,[15–17] and caudate.[10] Central to these findings is the idea that the subcortical regions (like the thalamus) are particularly affected early in the course of MS.[18–20] This early involvement may drive the subsequent changes of the rest of the brain, leading the brain switch towards unexpected states and causing reduced efficiency in high-order cognitive functions. However, current studies have not directly examined the effects that the subcortical regions have on driving network changes of the other parts of the brain, and cannot address the factors that make these subcortical regions exhibit changes early in MS, and especially in CIMS.

A key emerging approach that allows characterizing the extent to which brain regions can influence other parts of the brain is ‘network controllability’ analysis[21–23]. This approach allows us to move beyond determining whether there are changes in the functional connectivity of the brain, towards identifying which brain regions or networks are driving those changes and influencing the transition of brain states. Network controllability analysis has been validated as a powerful tool in exploring biomarkers in multiple neurological and neuropsychological diseases, including explaining the emergence of visual hallucinations in

Parkinson's Disease,[24] reflecting the genetic, individual and familial risk in major depressive disorder,[25] explaining psychopathological symptoms in schizophrenia,[26] and predicting positive syndrome in psychosis spectrum.[27] In MS, a relevant measure, the energy required by brain state transitions, has proven to be useful for distinguishing patients in different disability status.[28] However, whether network controllability measures alter in people with MS and whether these changes (if exist) differ between patients with different status of cognition remain unclear.

In this study, we aimed to investigate changes in brain network controllability and their associations with cognitive impairment in people with MS. To this end, we focused on the controllability measures that are most commonly applied in brain network analysis, and used them to study the controllability changes of static functional networks in MS. Subsequently, we compared the controllability of CIMS, CPMS and HC to explore potential biomarkers that differ between patients in different cognitive status. We hypothesize that: 1) MS patients show altered global controllability in a specific manner; 2) The controllability changes are concentrated predominantly within the subcortical network and particularly the thalamus that are highly relevant to cognitive function; and 3) are more pronounced in CIMS when compared to CPMS. Finally, an independent dataset was used to replicate our main results.

Materials and Methods

Participants

Main dataset

This dataset involved a total of 129 participants including 102 RRMS patients recruited from the Helen Durham Centre for Neuroinflammation at the University Hospital of Wales and 27 healthy controls (HC) recruited from the local community. All participants were aged between 18 and 60 years, right-handed, and devoid of contraindications for MR scanning. Additional eligibility criteria were required for the patients including the absence of comorbid neurological or psychiatric disease, no modifications to their treatments within three months prior to the MRI scanning, and being in a relapse-free phase. All participants underwent demographic information collection, clinical and psychological assessments, and MRI scanning in one study session. The main dataset study was approved by the NHS South-West Ethics and the Cardiff and Vale University Health Board R&D committees. Written informed

consent was obtained from each participant.

Replication dataset

To assess the reliability of our results, we replicated our analysis on a separate dataset from China. This dataset included 95 MS patients recruited from the Beijing Tiantan Hospital and 45 HC recruited from the local community. The participants were aged between 17 and 80 years, right-handed, and devoid of contraindications for MR scanning. Additional exclusion criteria were employed including incomplete MRI images, poor image quality, and a history of comorbid neurological or psychiatric disease. All participants underwent demographic information collection, clinical assessments, and MRI scanning in one study session after at least 4 weeks from any relapses. The replication dataset study was approved by the Institutional Review Board of the Beijing Tiantan Hospital, Capital Medical University, Beijing, China. Written informed consent was obtained from each participant.

Demographic, Clinical and Neuropsychological Assessment

Demographic and clinical data for both datasets included age, gender, education level, disease duration and the Expanded Disability Status Scale (EDSS) scores. The main dataset had additional clinical scores assessed using the Multiple Sclerosis Functional Composite (MSFC)[29] as well as cognitive scores assessed using the Brief Repeatable Battery of Neuropsychological Tests (BRB-N)[30] to measure the clinical function and cognitive performance of the patients.[30] The MSFC included the 25 Foot Walk Test (25-FWT), 9 Hole Peg Test (9-HPT), and Paced Auditory Serial Addition Task 3 seconds (PASAT3). The BRB-N consists of nine subtests which can be categorized into four cognitive domains according to previous studies:[31,32] 1) verbal memory: Selective Reminding Tests; 2) visual memory: 10/36 Spatial Recall Tests; 3) attention, information processing & executive function: Symbol Digit Modalities Test and Paced Auditory Serial Addition Tests; and 4) verbal fluency: Word List Generation Test. To quantify the extent of cognitive impairments in the patients from the main dataset, their scores on each subtest in BRB-N were transformed into Z-scores based on the mean and standard deviation (SD) values from the HC group. CIMS patients were defined as those who scored $\geq$ 1.5 SDs below the control mean on at least 2 subtests, while the other patients were considered as CPMS.[31,32] The score of each cognitive domain was calculated by averaging the scores of all subtests assigned in that domain. The global cognitive function score (global BRB-N) was calculated by averaging the scores of all four cognitive

domains.[31,32]

MRI Acquisition

Main dataset

MRI data were acquired on a 3T MR scanner (General Electric HDx MRI System, GE Medical Devices, Milwaukee, WI) with an 8-channel receive-only head radiofrequency coil. A high-resolution 3D T1-weighted sequence (3DT1) was acquired for identification of T1-hypointense MS lesions, segmentation, and registration (voxel size = 1 mm × 1 mm × 1 mm, echo time [TE] = 3.0 ms, repetition time [TR] = 7.8 ms, matrix size= 256 × 256 × 172, field of view [FOV] = 256 mm × 256 mm, flip angle (FA) = 20°). A T2/proton density–weighted sequence (voxel size = 0.94 mm × 0.94 mm × 4.5 mm, TE = 9.0/80.6 ms, TR = 3,000 ms, FOV = 240 mm × 240 mm, number of slices = 36, FA = 90°) and a fluid-attenuated inversion recovery (FLAIR) sequence (voxel size = 0.86 mm × 0.86 mm × 4.5 mm, TE = 122.3 ms, TR = 9,502 ms, FOV = 220 mm × 220 mm, number of slices = 36, FA = 90°) were acquired for identification and segmentation of T2-hyperintense MS lesions. Resting-state functional MRI (rs-fMRI) was acquired with a T2*-weighted gradient-echo echo-planar imaging sequence (voxel size = 3.4 mm × 3.4 mm × 3 mm, TE = 35 ms, TR = 3,000 ms, matrix size = 64 × 64 × 46, FOV = 220 mm × 220 mm, number of volumes = 100, number of slices = 46, interleaved order). All participants were instructed to relax with their eyes closed during rs-fMRI scanning.

Replication dataset

MRI data were acquired on a 3T MR scanner (Philips CX, Best, The Netherlands) including 3DT1, FLAIR, and rs-fMRI. 3DT1 image was acquired using sagittal acquisition with magnetization-prepared rapidly acquired gradient echo (voxel size = 1 mm × 1 mm × 1 mm, echo time [TE] = 3.0 ms, repetition time [TR] = 6.6 ms, matrix size = 196 × 256 × 170, inversion recovering = 880 ms, FA = 8°). FLAIR sequence was acquired using 3D sagittal acquisition with inversion recovering fast spin echo (voxel size = 1 mm × 1 mm × 1 mm, TE = 228 ms, TR = 4,800 ms, inversion time = 1650 ms, FA = 90°). rs-fMRI image was acquired using 2D axial acquisition with field echo EPI (voxel size = 3 mm × 3 mm × 3 mm, TE = 30 ms, TR = 2,000 ms, matrix size= 80 × 80 × 40, number of volumes = 180, number of slices = 40, interleaved order, slice thickness = 3 mm, slice gap = 0.3 mm, FA = 78°) during which all participants were instructed to relax with their eyes closed.

MRI preprocessing

Lesion filling was performed on the structural 3DT1 images of patients as previously described,[32] followed by segmentation into gray matter, white matter, and cerebrospinal fluid using SPM12 (v7771) toolbox (http://www.fil.ion.ucl.ac.uk/spm/software/spm12/). The quality of segmentation was assessed manually. rs-fMRI preprocessing was also performed by SPM12. Briefly, individual functional images were first corrected for head motion and acquisition time offsets between slices. No significant differences were found in the maximum and mean frame-wise displacement of head motion between groups in both the main and replication datasets ($p > 0.05$, permutation test). The corrected images were then spatially normalized to the MNI space by applying deformation fields derived from tissue segment of structural images. All normalized images further underwent spatial smoothing by a Gaussian kernel with 6-mm full width at half maximum.

Functional network construction

The functional network was constructed based on a combined parcellation scheme of 454 regions of interest (ROIs), including 400 cortical regions defined by the Schaefer atlas according to the functional network organization of cortical areas[33] and 54 subcortical regions defined by a subcortical parcellation derived from functional connectivity gradients of the subcortical areas.[34] We extracted and averaged the time series of each voxel within each ROI, and then calculated the Pearson correlation coefficient of the averaged time series between each ROI pair to characterize the functional connectivity. Spurious connections were excluded and only those connections with neurophysiological significance ($p < 0.05$) were preserved in the functional network.

Network control theory

Following previous studies[21,22], we constructed a simplified linear time-invariant control system to characterize the controllability of large scale functional brain networks. Specifically, we described the dynamics of brain state transitions as a linear time-invariant dynamical model of the form:

$$\dot{x}(t) = Ax(t) + Bu(t)$$

where $x(t)$ represents the brain state at time t; A is the time-invariant system matrix modelling the interactions between different nodes of the brain network and was defined as a

normalized version of the functional connectivity matrix; B is a matrix comprising columns of the identity matrix indicating the set of network nodes used to control the network; $u(t)$ denotes the input control energy injected at each control node at time t. To calculate A, we used a modified Laplacian normalization of the functional connectivity matrix F to ensure the stability of the dynamic system as described in a previous study.[22] Specifically, we calculated the Laplacian matrix as:

$$L_{ij} = \delta_{ij} \sum_{k=1}^{K} |F_{iK}| - F_{ij}$$

where F_{ij} is the (i, j) element of the functional matrix; K is the total number of nodes in the network; δ_{ij} is the Kronecker delta ($\delta_{ij} = 1$ if $i = j$ and $\delta_{ij} = 0$ otherwise). The functional connectivity matrix was then normalized into the system matrix as:

$$A = \frac{-L}{\lambda_{max}(L)}$$

with $\lambda_{max}(L)$ denoting the maximum absolute eigenvalue of the Laplacian matrix.

Network controllability measures

To characterize the ability of a given brain region (a network node) to control the whole network, we calculated the most widely used controllability measures for each brain region, including the average controllability, modal controllability and activation energy (Fig. 1).[21,22] The average controllability measures the ability of a node to drive the whole system towards easy-to-reach states (e.g. low energy states such as resting state activations), while the modal controllability measures the ability of a node to drive the whole system towards difficult-to-reach states (e.g. high energy states such as task-evoked activations). The activation energy measures the minimum control energy required to activate a given region under the dynamic control of the whole system. The average controllability of region i was calculated as the trace of the controllability Gramian matrix W_i, which is defined as

$$W_i = \int_0^{\infty} e^{At} B_i B_i^T e^{A^T t} dt$$

where e^{At} and $e^{A^T t}$ denote the matrix exponential of the matrices At and $A^T t$, respectively; B_i is the i-th column of the identity matrix, indicating that region i is used as control node. The modal controllability of region i was calculated as

$$\phi_i = \sum_{j=1}^{N} (1 - \lambda_j^2(A)) v_{ij}^2$$

with $\lambda_j(A)$ representing the j-th eigenvalue of the system matrix A, and $V = [v_{ij}]$ denoting the eigenvector matrix of A. The activation energy of region i was defined as

$$\varepsilon_i = \frac{1}{2} d_i^T W^{-1} d_i$$

where d_i is a column vector with the i-th element equal to one and the others being zero, indicating the activation of the i-th brain region.

Global, cortical, and subcortical controllability

To facilitate interpretation and comparison, ROI-level controllability measures were summarized at global (whole brain) and network levels. Global controllability measures were obtained by averaging each controllability measure across all the 454 ROIs. Cortical network controllability measures were obtained by averaging the controllability values of the 400 cortical ROIs into seven well-established cortical resting-state functional networks,[35] including the visual network (VN), somatomotor network (SMN), dorsal attention network (DAN), ventral attention network (VAN), limbic network (LN), frontoparietal network (FPN) and default mode network (DMN). The assignment between ROIs and functional networks was determined based on the maximum overlap between voxels of each ROI and each network. Similarly, subcortical network controllability measures were obtained by averaging the controllability values of the 54 subcortical ROIs into even well-known anatomical nuclei, namely, the hippocampus, thalamus, amygdala, caudate, nucleus accumbens, putamen and globus pallidus[34]. Additionally, the controllability of the subcortical network as a whole was characterized by averaging the controllability measures across all 54 subcortical ROIs.

Statistical analysis

Statistical analyses were performed using MATLAB software version R2022b (MathWorks, Inc). Chi-squared tests were used to compare dichotomous variables (gender). The group comparisons of continuous demographic, clinical and neuropsychological variables were performed by permutation tests (10,000 times). Age and gender were considered as covariates for the neuropsychological variables. A 95% confidence interval was used for each effect.

Assessment of global, cortical, and subcortical controllability changes in MS

The differences on global, cortical, and subcortical controllability between MS and HC were

identified by permutation tests (10,000 times). Age and gender were considered as covariates. An additional model that controlled for age, gender and education level was also tested. FDR correction was used for multiple comparisons. Notably, any controllability measures that exceeded 1.5 times the interquartile range above quartile 3 or fell below 1.5 times the interquartile range beneath quartile 1 within each group were identified as outliers and then replaced with their nearest non-outlier values before comparisons. To test the reliability of our results, we further assessed controllability changes in MS in the replication dataset. All analysis procedures were performed identically between the two datasets.

Assessment of controllability changes in CIMS and CPMS

To explore how controllability changes relate to cognitive impairment in MS, we further assessed controllability changes in CIMS and CPMS from the main dataset. Specifically, permutation tests (10,000 times) were first applied between CIMS, CPMS and HC. For those controllability measures that showed significant differences among the three groups after FDR correction, *post hoc* tests were further used for the pairwise comparisons between each two groups. Again, age and gender were considered as covariates. The model that additionally controlled for education level was also tested. Outliers of controllability measures were replaced as described before.

Association between changed controllability measures and clinical/neuropsychological variables

Correlation analyses were performed between changed controllability measures and clinical/neuropsychological variables in MS. Partial Pearson correlation coefficients were calculated between changed controllability measures and neuropsychological test scores as well as disease duration and MSFC test scores, while partial Spearman correlation coefficients were evaluated between changed controllability measures and EDSS scores. Age and gender were considered as covariates of no interest. FDR corrections were performed for multiple comparisons.

Data availability

The data that support the results of this study are available from the corresponding author upon reasonable request and with permission.

Results

Demographic, clinical, and neuropsychological characteristics

Main dataset

Table 1 summarizes the demographic, clinical and neuropsychological information of the participants. While there were no group differences in gender distribution ($p > 0.05$), the MS group were significantly older ($p = 0.012$) and had lower education levels ($p < 0.001$) than the HCs. Moreover, the MS group exhibited worse performance on all subtests of the MSFC (25-FWT, $p = 0.003$; 9-HPT, $p < 0.001$; PASAT3, $p < 0.001$) than the HC group. When performing group comparisons on the cognitive scores, the MS group showed worse performance than HCs on all four cognitive domains (verbal memory, $p = 0.002$; visual memory, $p = 0.020$; attention, information processing and executive, $p < 0.001$; verbal fluency, $p = 0.031$), as well as the global BRB-N ($p < 0.001$).

In order to assess the association between controllability changes and cognitive impairment, the MS group was further split into CIMS and CPMS subgroups. Among the 102 MS patients, 55 were identified as CIMS and 47 as CPMS. No significant differences in gender distribution ($p > 0.05$), disease duration ($p > 0.05$) or EDSS score ($p > 0.05$) were found between the two MS subgroups. However, further comparisons with HC revealed older age in CIMS than HC ($p = 0.004$) and lower education level in both CIMS ($p < 0.001$) and CPMS ($p < 0.001$) than HC. Additionally, CPMS showed lower score on 9-HPT than HC ($p = 0.018$), while CIMS showed worse performance on 25-FWT ($p < 0.001$) than HC, and worse performance on 9-HPT and PASAT3 than both CPMS ($p = 0.033$ / $p < 0.001$) and HC ($p < 0.001$ / $p < 0.001$). For the neuropsychological tests, CIMS showed worse performance than both CPMS and HC on all four cognitive domains ($p < 0.001$) as well as on the global BRB-N score ($p < 0.001$). No differences were found between CPMS and HC on any of the cognitive measures ($p > 0.05$).

Replication dataset

The demographic and clinical information of the participants are shown in Supplementary Table 1. The MS group was significantly younger ($p = 0.014$) and had lower education level ($p = 0.004$) than the HC group. No differences were found in gender distribution between MS and HC ($p > 0.05$). Due to the inconsistency in the cognitive assessment scales between the replication and the main datasets, further subgroup splitting and analysis in terms of CIMS

and CPMS were not available on the replication dataset.

Global, cortical, and subcortical controllability changes in MS

Main dataset

For global controllability, MS group showed increased average controllability ($p < 0.001$) but decreased modal controllability ($p = 0.008$) and decreased activation energy ($p = 0.016$) compared to HC group (Supplementary Fig. 1A). For controllability of the seven cortical networks, MS group showed increased average controllability in the VN ($p = 0.005$), SMN ($p < 0.001$), DAN ($p < 0.001$), VAN ($p = 0.002$), FPN ($p < 0.001$), and DMN ($p = 0.005$) compared to HC group (Supplementary Fig. 2A and 2B). For controllability of the subcortical network as a whole, MS group exhibited increased average controllability ($p = 0.001$) but decreased modal controllability ($p = 0.002$) as well as decreased activation energy ($p < 0.001$) compared to HC group (Fig. 2A). For controllability of the seven subcortical nuclei, MS group showed increased average controllability ($p < 0.001$) but decreased modal controllability ($p = 0.005$) as well as decreased activation energy ($p = 0.007$) in the thalamus compared to HC group (Fig. 3A). Besides, decreased activation energy in the globus pallidus ($p = 0.004$) was also found in MS group (Fig. 3B). The pattern of results remained the same after models were controlled for education level.

Replication dataset

No difference was found in global and cortical controllability between MS and HC. For controllability of the subcortical network as a whole, MS group exhibited replicated increased average controllability ($p = 0.005$) when compared to HC group (Fig. 2B). For controllability of the seven subcortical nuclei, MS group showed replicated increased average controllability in the thalamus when compared to HC group ($p = 0.027$, Fig. 3C). Besides, increased average controllability was also found in the caudate, nucleus accumbens and putamen in MS when compared to HC ($p < 0.05$, Supplementary Fig. 3).

Controllability changes in CIMS and CPMS

Main dataset

For global controllability, both CIMS and CPMS showed increased average controllability (CIMS vs. HC: $p = 0.002$; CPMS vs. HC: $p < 0.001$), while CIMS additionally exhibited decreased modal controllability ($p = 0.009$) and decreased activation energy ($p = 0.016$),

when compared to HC. No difference was found between CIMS and CPMS (Supplementary Fig. 1B). For controllability of the seven cortical networks, both CIMS and CPMS showed increased average controllability in the VN (CIMS vs. HC: $p = 0.011$; CPMS vs. HC: $p = 0.005$), SMN (CIMS vs. HC: $p = 0.002$; CPMS vs. HC: $p = 0.002$), DAN (CIMS vs. HC: $p = 0.001$; CPMS vs. HC: $p < 0.001$), VAN (CIMS vs. HC: $p = 0.016$; CPMS vs. HC: $p = 0.002$), FPN (CIMS vs. HC: $p = 0.001$; CPMS vs. HC: $p = 0.003$) and DMN (CIMS vs. HC: $p = 0.015$; CPMS vs. HC: $p = 0.001$) compared to HC. No difference was found between CIMS and CPMS (Supplementary Fig. 2A and 2C). For controllability of the subcortical network as a whole, both CIMS and CPMS showed increased average controllability (CIMS vs. HC: $p < 0.001$; CPMS vs. HC: $p = 0.008$) but decreased modal controllability (CIMS vs. HC: $p = 0.006$; CPMS vs. HC: $p = 0.008$) and decreased activation energy (CIMS vs. HC: $p = 0.007$; CPMS vs. HC: $p = 0.003$) when compared to HC. No difference was found between CIMS and CPMS (Fig. 4). For controllability of the seven subcortical nuclei, both CIMS and CPMS showed increased average controllability in the thalamus (CIMS vs. HC: $p < 0.001$; CPMS vs. HC: $p = 0.009$; Fig. 5A) as well as decreased activation energy in the globus pallidus (CIMS vs. HC: $p = 0.010$; CPMS vs. HC: $p = 0.007$; Fig. 5B) compared to HC. Additionally, the CIMS group showed decreased modal controllability ($p = 0.002$) and activation energy ($p = 0.006$) in the thalamus (Fig. 5A). When comparing between the patient subgroups, CIMS exhibited higher average controllability than CPMS in the thalamus ($p = 0.016$, Fig. 5A). The pattern of results remained the same after models were controlled for education level.

Correlation between changed controllability measures and clinical/neuropsychological variables

No statistically significant correlations were observed between the controllability measures and any of the clinical or neuropsychological variables after FDR correction.

Discussion

In this study, we investigated network controllability changes in MS to identify whether there are networks or brain regions in people with MS that play a specific role in driving network changes and state transitions across the brain. We then linked these controllability changes to the cognitive status in patients. Our results showed that people with MS present global changes on all three of the main controllability measures, which were concentrated predominantly within the subcortical network, particularly in the thalamus. These results

were further confirmed by the replication dataset. Subsequent comparisons between CIMS, CPMS and HC groups demonstrated consistent results, where CIMS further showed greater controllability changes within the thalamus than CPMS. Our study therefore reveals a specific controllability pattern that highlights alterations in the involvement of the subcortical network and particularly the thalamus in driving network changes and state transitions in MS and CIMS, suggesting a possible brain mechanism underpinning cognitive impairment in this disease.

The observed changes in resting state network controllability in this work are consistent with previous studies reporting alterations in brain state dynamics in MS; for example, altered dwell time of specific brain states and frequency of transitions between states during resting state conditions.[8,36] The present work, however, extends previous studies by elucidating potential mechanisms in which the MS pathology disturbed the dynamics of brain states. The controllability measures used in this study described the effect of a network or region on driving state transition from different aspects. Specifically, average controllability identifies regions that contribute more to brain transitions towards easy-to-reach states like the resting state.[21,22,37] Functional hubs with denser or stronger connections typically exhibit higher average controllability. These regions have close connection with multiple regions throughout the brain and contribute to transition between states that require lower energy costs.[22,38] Modal controllability identifies regions that mainly facilitate brain transitions towards difficult-to-reach states, such as cognitive task states.[21,22,37] Regions with higher modal controllability seem to be located avoiding hubs. These regions have sparser or weaker connections with the others and contribute to transition that require higher energy costs.[22,38] Regional activation energy describes the minimum input energy required to activate a specific region, in the context that all regions contribute collectively to driving this activation. Regions with lower activation energy are easier to be activated.[22,39] Our findings revealed that people with MS exhibited increased average controllability but decreased modal controllability and decreased activation energy. The changes of each controllability measure followed a consistent direction regardless of whether we examined them in global or any cortical or subcortical networks. This implies that MS pathology does not cause random changes in brain state transitions: instead, it causes a special changing pattern across the brain, specifically resulting in facilitating transitions towards easy-to-reach states while making transitions towards hard-to-reach states more costly.

Our results revealed a selective vulnerability of controllability alteration in MS, wherein the subcortical network and its thalamus exhibited the most pronounced

controllability changes among the whole brain, which were further confirmed by an independent dataset. In resting-state functional network of the healthy brain, the subcortical network plays a crucial role in controlling the dynamics of brain function. It contributes the most to transitions between easy-to-reach brain states while the least to transitions between difficult-to-reach brain states among the whole brain in health cohorts.[22] In our study, the subcortical network in healthy controls fit this pattern. However interestingly, MS pathology seemed to further exacerbate the extremes of the two types of controllability. That is, in MS, the highest subcortical average controllability further increased, while the lowest subcortical modal controllability further decreased. The subcortical regions have proven to be the first and most vulnerable parts to disease attacks across the whole brain in MS.[18–20] Therefore, one possible mechanism underlying the imbalanced subcortical controllability in MS might be due to an early compensation strategy against the disease, which prioritizes the preservation of transitions towards fundamental brain states (such as the easy-to-reach resting state) while relinquishing transitions towards high-order states (such as the difficult-to-reach cognitive task state). This might further relate to the subsequent development of high-order cognitive dysfunction in patients with this disease.

The analysis of cognitive subgroups further supported this view that controllability changes may impact on cognition. While both CIMS and CPMS showed controllability changes compared to HC, the thalamus in CIMS showed significantly greater increase in average controllability than CPMS. This indicated in people with CIMS, the thalamus exhibited an exceeded facilitation of transitions towards easy-to-reach states. As a key hub with strong connections across the brain and playing a significant role in human cognition, the thalamus has gained considerable attention in MS, and has proven to highly relate to cognitive impairment in MS patients.[9,13,14,40–48] Several studies consistently observed higher thalamic functional connectivity in CIMS when compared to CPMS.[11,13,14] Furthermore, the thalamus specifically demonstrates neurodegeneration and atrophy in the early course of MS,[18,19] meanwhile its structure and function were reported to determine the severity of cognitive impairment in MS patients.[11,47] These findings strongly implicate thalamic changes as promising biomarkers for cognitive dysfunction in people with MS. Despite the lack of previous studies exploring network controllability changes in cognitive impairment in MS, network controllability measures have already been recognized as a powerful tool to identify disease-related changes in various conditions[24–27] and explain cognitive performance in both health and disease.[22,49–51] Our present study originally explored network controllability alterations in MS, and revealed the specific effect that the subcortical network and

particularly the thalamus has on driving network changes across the whole brain in MS and CIMS. Notably, a recent longitudinal study in MS has reported that the deep gray matter regions, including the thalamus, drive the worsening of disability in the patients.[52] This suggests that the controllability changes in the subcortical network, especially in the thalamus, could potentially signify an early mechanism underpinning cognitive decline, and may drive the worsening of cognitive dysfunction in MS. Future longitudinal studies with large cohort of CIMS and sophisticated analytical techniques with attention to temporal profiles of the network controllability and cognitive dysfunction in patients may allow us to test this hypothesis.

This study has several limitations. First, while the CIMS and CPMS groups were matched for age and gender, the whole MS group displayed an older age than the HC group. To mitigate the impact of demographic disparities on the results, we included age and gender as covariates in our statistical models. Second, although we observed replicated controllability changes in MS in the subcortical network and the thalamus from two independent datasets, the global and cortical controllability changes observed in the main dataset were not observed in the replication dataset. This could be due to more heterogeneous controllability changes throughout the cortex. Third, while we found controllability difference between CIMS and CPMS, no significant associations were found between the changed controllability and cognitive performance in the patients after FDR correction. Future studies with multiple imaging modalities may provide a more comprehensive explanation of cognitive impairment in MS. Finally, this study is a cross-sectional investigation of brain controllability changes in MS, future studies employing longitudinal designs should be conducted to explore whether and how controllability changes exacerbate the progression of cognitive impairment in MS.

Conclusion

This study shows the specific effect that the subcortical network and the thalamus has on driving network changes and its association with cognitive impairment in MS. Our results emphasize the crucial role of the subcortical network and the thalamus in preserving brain transitions towards easy-to-reach network states while relinquishing brain transitions towards difficult-to-reach network states in MS, especially in CIMS, suggesting a possible brain mechanism underpinning the emergence of cognitive impairment in individuals with MS.

Acknowledgements

The authors express their gratitude to Dr. Danka Jandric, Dr. Elizabeth McManus, Dr. Caroline Lea-Carnall, Megan Sheppard, Katie Moran, Marta Litwinczuk, Sasha Johns, and Vanesa Benuskova for their valuable support during this study.

Funding

This study was supported by the Guangzhou overseas elite scholarship council of China (GESC).

Competing interests

The authors report no competing interests.

Supplementary material

Supplementary material is available at *bioRxiv* online.

References

1. Chiaravalloti ND, DeLuca J. Cognitive impairment in multiple sclerosis. *The Lancet Neurology*. 2008;7(12):1139-1151. doi:10.1016/S1474-4422(08)70259-X

2. Benedict RHB, Amato MP, DeLuca J, Geurts JJG. Cognitive impairment in multiple sclerosis: clinical management, MRI, and therapeutic avenues. *The Lancet Neurology*. 2020;19(10):860-871. doi:10.1016/S1474-4422(20)30277-5

3. Eijlers AJC, Meijer KA, Wassenaar TM, et al. Increased default-mode network centrality in cognitively impaired multiple sclerosis patients. *Neurology*. 2017;88(10):952-960. doi:10.1212/WNL.0000000000003689

4. Eijlers AJC, Wink AM, Meijer KA, Douw L, Geurts JJG, Schoonheim MM. Reduced Network Dynamics on Functional MRI Signals Cognitive Impairment in Multiple Sclerosis. *Radiology*. 2019;292(2):449-457. doi:10.1148/radiol.2019182623

5. Meijer KA, Eijlers AJC, Douw L, et al. Increased connectivity of hub networks and cognitive impairment in multiple sclerosis. *Neurology*. 2017;88(22):2107-2114. doi:10.1212/WNL.0000000000003982

6. Rocca MA, Valsasina P, Absinta M, et al. Default-mode network dysfunction and cognitive impairment in progressive MS. *Neurology*. 2010;74(16):1252-1259. doi:10.1212/WNL.0b013e3181d9ed91

7. Hidalgo de la Cruz M, Valsasina P, Sangalli F, Esposito F, Rocca MA, Filippi M. Dynamic Functional Connectivity in the Main Clinical Phenotypes of Multiple Sclerosis. *Brain Connect*. 2021;11(8):678-690. doi:10.1089/brain.2020.0920

8. d'Ambrosio A, Valsasina P, Gallo A, et al. Reduced dynamics of functional connectivity and cognitive impairment in multiple sclerosis. *Mult Scler*. 2020;26(4):476-488. doi:10.1177/1352458519837707

9. Tona F, Petsas N, Sbardella E, et al. Multiple sclerosis: altered thalamic resting-state functional connectivity and its effect on cognitive function. *Radiology*. 2014;271(3):814-821. doi:10.1148/radiol.14131688

10. Cruz-Gómez ÁJ, Aguirre N, Sanchis-Segura C, Ávila C, Forn C. Subcortical grey matter structures in multiple sclerosis: what is their role in cognition? *Neuroreport*. 2018;29(7):547-552. doi:10.1097/WNR.0000000000000976

11. Schoonheim MM, Hulst HE, Brandt RB, et al. Thalamus structure and function determine severity of cognitive impairment in multiple sclerosis. *Neurology*. 2015;84(8):776-783. doi:10.1212/WNL.0000000000001285

12. Rocca MA, Valsasina P, Meani A, Falini A, Comi G, Filippi M. Impaired functional integration in multiple sclerosis: a graph theory study. *Brain Struct Funct*. 2016;221(1):115-131. doi:10.1007/s00429-014-0896-4

13. d'Ambrosio A, Hidalgo de la Cruz M, Valsasina P, et al. Structural connectivity-defined thalamic subregions have different functional connectivity abnormalities in multiple

sclerosis patients: Implications for clinical correlations. *Hum Brain Mapp*. 2017;38(12):6005-6018. doi:10.1002/hbm.23805

14. Rocca MA, Valsasina P, Leavitt VM, et al. Functional network connectivity abnormalities in multiple sclerosis: Correlations with disability and cognitive impairment. *Mult Scler*. 2018;24(4):459-471. doi:10.1177/1352458517699875

15. Roosendaal SD, Hulst HE, Vrenken H, et al. Structural and Functional Hippocampal Changes in Multiple Sclerosis Patients with Intact Memory Function. *Radiology*. 2010;255(2):595-604. doi:10.1148/radiol.10091433

16. Hulst HE, Schoonheim MM, Van Geest Q, Uitdehaag BMJ, Barkhof F, Geurts JJG. Memory impairment in multiple sclerosis: Relevance of hippocampal activation and hippocampal connectivity. *Mult Scler*. 2015;21(13):1705-1712. doi:10.1177/1352458514567727

17. Karavasilis E, Christidi F, Velonakis G, et al. Hippocampal structural and functional integrity in multiple sclerosis patients with or without memory impairment: a multimodal neuroimaging study. *Brain Imaging and Behavior*. 2019;13(4):1049-1059. doi:10.1007/s11682-018-9924-y

18. Coupé P, Planche V, Mansencal B, et al. Lifespan neurodegeneration of the human brain in multiple sclerosis. *Human Brain Mapping*. 2023;n/a(n/a). doi:10.1002/hbm.26464

19. Eshaghi A, Marinescu RV, Young AL, et al. Progression of regional grey matter atrophy in multiple sclerosis. *Brain*. 2018;141(6):1665-1677. doi:10.1093/brain/awy088

20. Tozlu C, Olafson E, Jamison K, et al. The sequence of regional structural disconnectivity due to multiple sclerosis lesions. *bioRxiv*. Published online January 27, 2023:2023.01.26.525537. doi:10.1101/2023.01.26.525537

21. Gu S, Pasqualetti F, Cieslak M, et al. Controllability of structural brain networks. *Nat Commun*. 2015;6(1):8414. doi:10.1038/ncomms9414

22. Deng S, Li J, Thomas Yeo BT, Gu S. Control theory illustrates the energy efficiency in the dynamic reconfiguration of functional connectivity. *Commun Biol*. 2022;5(1):295. doi:10.1038/s42003-022-03196-0

23. Lynn CW, Bassett DS. The physics of brain network structure, function and control. *Nat Rev Phys*. 2019;1(5):318-332. doi:10.1038/s42254-019-0040-8

24. Zarkali A, McColgan P, Ryten M, et al. Differences in network controllability and regional gene expression underlie hallucinations in Parkinson's disease. *Brain*. 2020;143(11):3435-3448. doi:10.1093/brain/awaa270

25. Hahn T, Winter NR, Ernsting J, et al. Genetic, individual, and familial risk correlates of brain network controllability in major depressive disorder. *Mol Psychiatry*. Published online January 13, 2023. doi:10.1038/s41380-022-01936-6

26. Li Q, Yao L, You W, et al. Controllability of Functional Brain Networks and Its Clinical Significance in First-Episode Schizophrenia. *Schizophrenia Bulletin*. 2023;49(3):659-668. doi:10.1093/schbul/sbac177

27. Parkes L, Moore TM, Calkins ME, et al. Network controllability in transmodal cortex predicts positive psychosis spectrum symptoms. *Biol Psychiatry*. 2021;90(6):409-418. doi:10.1016/j.biopsych.2021.03.016

28. Tozlu C. Larger lesion volume in people with multiple sclerosis is associated with increased transition energies between brain states and decreased entropy of brain activity.pdf. *Network Neuroscience*. Published online 2022. doi:https://doi.org/10.1162/netn_a_00292

29. Cutter GR, Baier ML, Rudick RA, et al. Development of a multiple sclerosis functional composite as a clinical trial outcome measure. *Brain*. 1999;122 (Pt 5):871-882. doi:10.1093/brain/122.5.871

30. Amato MP, Portaccio E, Goretti B, et al. The Rao's Brief Repeatable Battery and Stroop test: normative values with age, education and gender corrections in an Italian population. *Mult Scler*. 2006;12(6):787-793. doi:10.1177/1352458506070933

31. Sepulcre J, Vanotti S, Hernández R, et al. Cognitive impairment in patients with multiple sclerosis using the Brief Repeatable Battery-Neuropsychology test. *Mult Scler*. 2006;12(2):187-195. doi:10.1191/1352458506ms1258oa

32. Jandric D, Lipp I, Paling D, et al. Mechanisms of Network Changes in Cognitive Impairment in Multiple Sclerosis. *Neurology*. 2021;97(19):e1886-e1897. doi:10.1212/WNL.0000000000012834

33. Schaefer A, Kong R, Gordon EM, et al. Local-Global Parcellation of the Human Cerebral Cortex from Intrinsic Functional Connectivity MRI. *Cerebral Cortex*. 2018;28(9):3095-3114. doi:10.1093/cercor/bhx179

34. Tian Y, Margulies DS, Breakspear M, Zalesky A. Topographic organization of the human subcortex unveiled with functional connectivity gradients. *Nat Neurosci*. 2020;23(11):1421-1432. doi:10.1038/s41593-020-00711-6

35. Yeo BTT, Krienen FM, Sepulcre J, et al. The organization of the human cerebral cortex estimated by intrinsic functional connectivity. *Journal of Neurophysiology*. 2011;106(3):1125-1165. doi:10.1152/jn.00338.2011

36. Romanello A, Krohn S, von Schwanenflug N, et al. Functional connectivity dynamics reflect disability and multi-domain clinical impairment in patients with relapsing-remitting multiple sclerosis. *NeuroImage: Clinical*. 2022;36:103203. doi:10.1016/j.nicl.2022.103203

37. Pasqualetti F, Zampieri S, Bullo F. Controllability Metrics, Limitations and Algorithms for Complex Networks.

38. Deng S, Gu S. Controllability Analysis of Functional Brain Networks. Published online March 18, 2020. doi:10.48550/arXiv.2003.08278

39. Gu S, Betzel RF, Mattar MG, et al. Optimal trajectories of brain state transitions. *NeuroImage*. 2017;148:305-317. doi:10.1016/j.neuroimage.2017.01.003

40. Šteckova T, Hluštík P, Sládková V, Odstrčil F, Mareš J, Kaňovský P. Thalamic atrophy

and cognitive impairment in clinically isolated syndrome and multiple sclerosis. *Journal of the Neurological Sciences*. 2014;342(1):62-68. doi:10.1016/j.jns.2014.04.026

41. Amin M, Ontaneda D. Thalamic Injury and Cognition in Multiple Sclerosis. *Frontiers in Neurology*. 2021;11. Accessed October 27, 2023. https://www.frontiersin.org/articles/10.3389/fneur.2020.623914

42. Houtchens MK, Benedict RHB, Killiany R, et al. Thalamic atrophy and cognition in multiple sclerosis. *Neurology*. 2007;69(12):1213-1223. doi:10.1212/01.wnl.0000276992.17011.b5

43. Batista S, Zivadinov R, Hoogs M, et al. Basal ganglia, thalamus and neocortical atrophy predicting slowed cognitive processing in multiple sclerosis. *J Neurol*. 2012;259(1):139-146. doi:10.1007/s00415-011-6147-1

44. Bisecco A, Capuano R, Caiazzo G, et al. Regional changes in thalamic shape and volume are related to cognitive performance in multiple sclerosis. *Mult Scler*. 2021;27(1):134-138. doi:10.1177/1352458519892552

45. Conway DS, Planchon SM, Oh SH, et al. Measures of Thalamic Integrity are Associated with Cognitive Functioning in Fingolimod-treated Multiple Sclerosis Patients. *Multiple Sclerosis and Related Disorders*. 2021;47:102635. doi:10.1016/j.msard.2020.102635

46. Sandroff BM, Motl RW, Román CAF, et al. Thalamic atrophy moderates associations among aerobic fitness, cognitive processing speed, and walking endurance in persons with multiple sclerosis. *J Neurol*. 2022;269(10):5531-5540. doi:10.1007/s00415-022-11205-9

47. Lorefice L, Carta E, Frau J, et al. The impact of deep grey matter volume on cognition in multiple sclerosis. *Multiple Sclerosis and Related Disorders*. 2020;45:102351. doi:10.1016/j.msard.2020.102351

48. Jandric D, Doshi A, Scott R, et al. A Systematic Review of Resting-State Functional MRI Connectivity Changes and Cognitive Impairment in Multiple Sclerosis. *Brain Connectivity*. Published online 2022:brain.2021.0104. doi:10.1089/brain.2021.0104

49. Lee WH, Rodrigue A, Glahn DC, Bassett DS, Frangou S. Heritability and Cognitive Relevance of Structural Brain Controllability. *Cereb Cortex*. 2020;30(5):3044-3054. doi:10.1093/cercor/bhz293

50. Cui Z, Stiso J, Baum GL, et al. Optimization of energy state transition trajectory supports the development of executive function during youth. Yeo T, Behrens TE, eds. *eLife*. 2020;9:e53060. doi:10.7554/eLife.53060

51. Braun U, Harneit A, Pergola G, et al. Brain network dynamics during working memory are modulated by dopamine and diminished in schizophrenia. *Nat Commun*. 2021;12(1):3478. doi:10.1038/s41467-021-23694-9

52. Eshaghi A, Prados F, Brownlee WJ, et al. Deep gray matter volume loss drives disability worsening in multiple sclerosis. *Ann Neurol*. 2018;83(2):210-222. doi:10.1002/ana.25145

53. Xia M, Wang J, He Y. BrainNet Viewer: A Network Visualization Tool for Human Brain

Connectomics. *PLOS ONE*. 2013;8(7):e68910. doi:10.1371/journal.pone.0068910

54. Wang J, Wang X, Xia M, Liao X, Evans A, He Y. GRETNA: a graph theoretical network analysis toolbox for imaging connectomics. *Front Hum Neurosci*. 2015;9. doi:10.3389/fnhum.2015.00386

Table 1. Demographic, clinical, and neuropsychological variables from the main dataset

	HC (n = 27)	**MS (n = 102)**	***p* value (HC vs MS)**	**CPMS (n = 47)**	**CIMS (n = 55)**	***p* value (HC vs CPMS vs CIMS**
Age, y	37 (23-59)	45 (18-60)	0.012	42 (18-60)	47 (20-60)	0.012[b]
Gender, n (female/male)	15/12	69/33	0.241	36/11	33/22	0.108
Education, y	19 (12-30)	15 (10-30)	< 0.001	15 (10-27)	14 (10-30)	< 0.001[b, c]
Disease duration, y	-	12 (1-39)	-	12 (2-37)	11.5 (1-39)	0.794
EDSS	-	4.0 (0-6.5)	-	4.0 (0-6)	4.0 (0-6.5)	0.251
MSFC						
25-FWT	4.35 (3.20-5.40)	5.25 (3.60-26.80)	0.003	5.15 (3.70-12.95)	5.43 (3.60-26.80)	0.002[b]
9-HPT	18.65 (15.35-23.00)	21.75 (16.35-59.50)	< 0.001	21.45 (17.15-44.85)	21.95 (16.35-59.50)	< 0.001[a,b,c]
PASAT3	51.00 (35.00-59.00)	43.50 (0-60.00)	< 0.001	50.00 (30.00-60.00)	34.00 (0-58.00)	< 0.001[a,b]
BRB-N						
Verbal memory	36.33 (21.33-47.33)	29.17 (4.00-48.33)	0.002	36.00 (22.33-48.33)	23.00 (4.00-47.33)	< 0.001[a,b]
Visual memory	7.83 (4.50-9.50)	6.17 (2.67-9.67)	0.020	7.33 (4.67-9.67)	5.33 (2.67-9.33)	< 0.001[a,b]
Information processing, attention, executive function	50.67 (36.33-62.67)	41.83 (12.67-58.00)	< 0.001	46.67 (36.67-58.00)	34.67 (12.67-56.67)	< 0.001[a,b]
Verbal fluency	29.00 (13.00-44.00)	27.00 (7.00-42.00)	0.031	29.00 (19.00-42.00)	24.00 (7.00-40.00)	< 0.001[a,b]
Global BRB-N	33.78 (26.56-42.52)	27.85 (8.56-38.59)	< 0.001	32.74 (26.00-38.59)	23.62 (8.56-35.22)	< 0.001[a,b]

Data are represented as median (range) except for gender ratio (female/male). HC = healthy controls; MS = multiple sclerosis; CPMS = cognitively preserved MS; CIMS = cognitively impaired MS; EDSS = Expanded Disability Status Scale; MSFC = Multiple Sclerosis Functional Composite; 25-FWT = 25 Foot Walk Test; 9-HPT = 9 Hole Peg Test; PASAT3 = Paced Auditory Serial Addition Task 3 seconds. BRB-N = Brief Repeatable Battery of Neuropsychological Tests.

[a] Significant difference between the CIMS and CPMS.

[b] Significant difference between the CIMS and HC.

[c] Significant difference between the CPMS and HC.

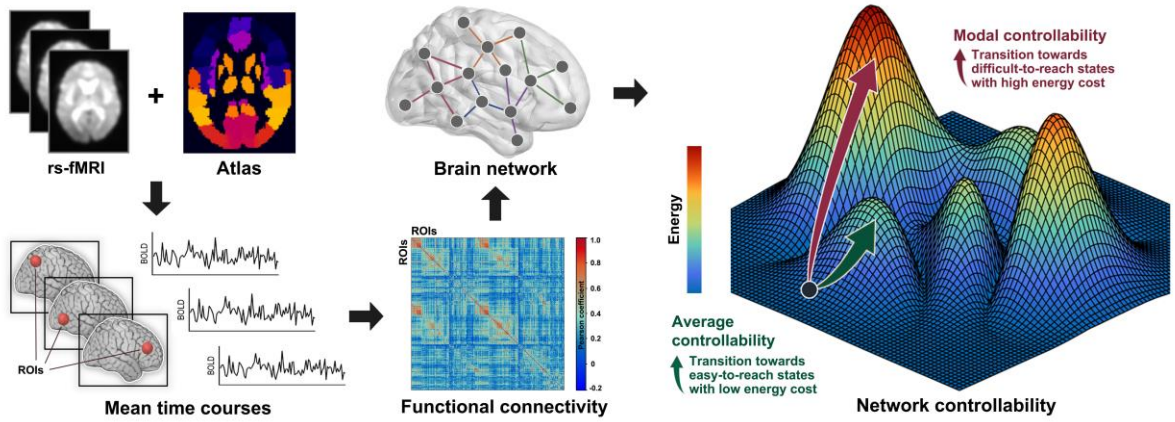

Figure 1. Overview of the controllability calculation. Based on rs-fMRI data from 129 participants and the combined cortical and subcortical parcellations, we extracted regional mean time courses and calculated the functional connectivity between region pairs to construct the brain network. Subsequently, we calculated the controllability measures that are most commonly applied in brain network analysis. These measures include average controllability, which characterizes contributions to transitions towards easy-to-reach states with low energy cost; modal controllability, which characterizes contributions to transitions towards difficult-to-reach states with high energy cost; and activation energy, which characterizes the minimum energy required to activate a specific region under the control of the whole brain network.

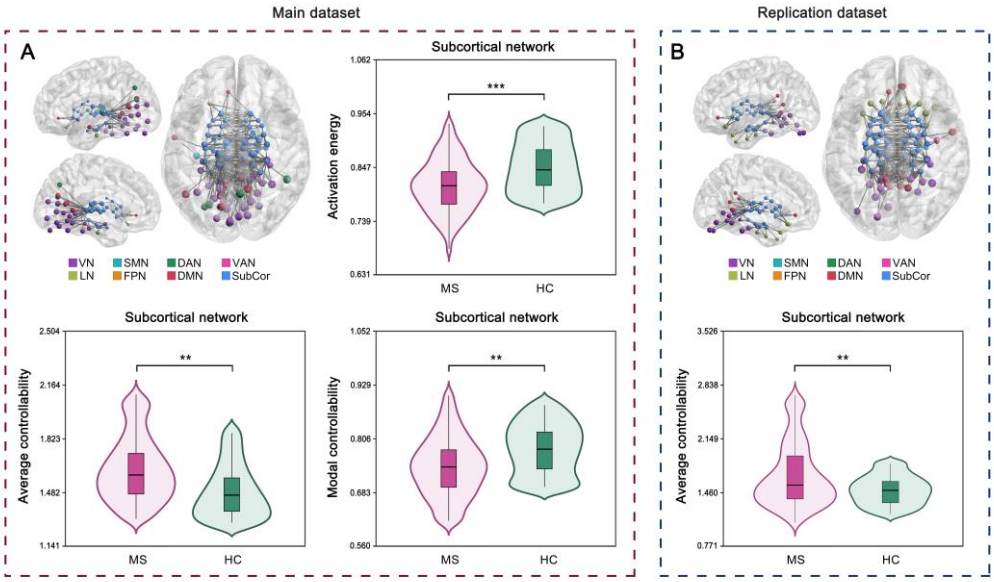

Figure 2. Controllability changes in the subcortical network in MS from the main and replication datasets. (A) Increased average controllability but decreased modal controllability and decreased activation energy in the subcortical network in MS from the main dataset. (B) Replicated increased average controllability in the subcortical network in MS from the replication dataset. Brain network visualizations were generated using BrainNet Viewer[53], violin plots were generated using GRETNA[54]. SubCor = subcortical network; $^{*}p < 0.050$; $^{**}p < 0.010$; $^{***}p < 0.001$.

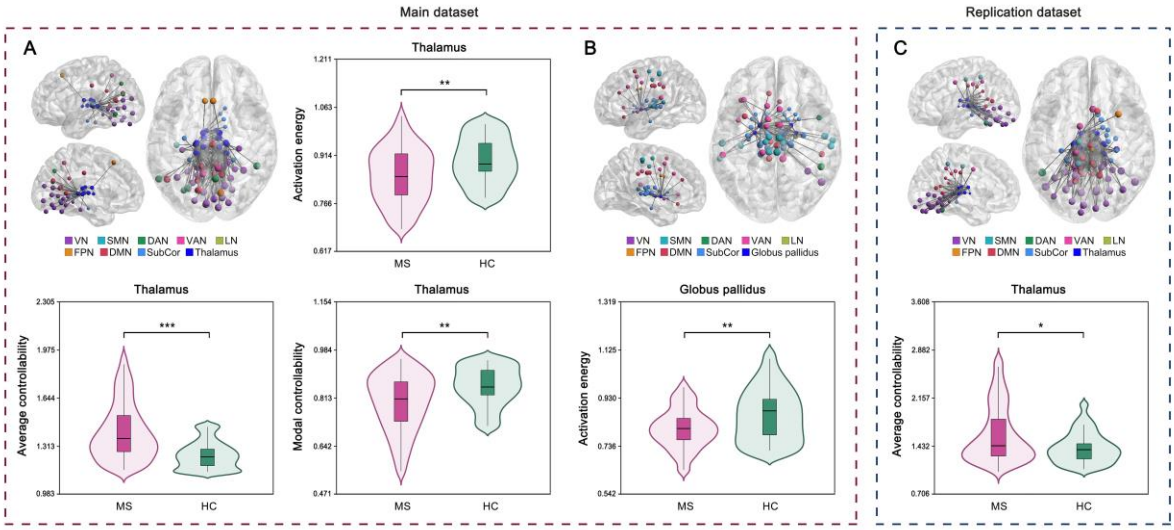

Figure 3. Controllability changes in the subcortical nuclei in MS from the main and replication datasets. (A) Increased average controllability but decreased modal controllability and decreased activation energy in the thalamus in MS from the main dataset. (B) Decreased activation energy in the globus pallidus in MS from the main dataset. (C) Replicated increased average controllability in the thalamus in MS from the replication dataset. SubCor = subcortical network; $^{*}p < 0.050$; $^{**}p < 0.010$; $^{***}p < 0.001$.

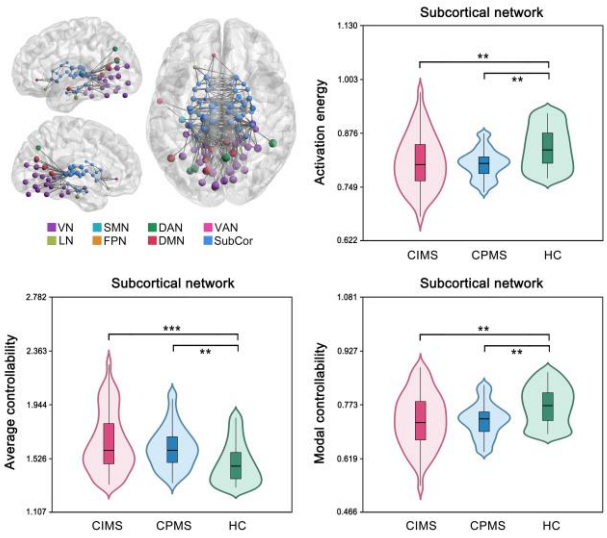

Figure 4. Controllability changes in the subcortical network in CIMS and CPMS.

Increased average controllability but decreased modal controllability and decreased activation energy in the subcortical network in both CIMS and CPMS when compared to HC. SubCor = subcortical network; $^{*}p < 0.050$; $^{**}p < 0.010$; $^{***}p < 0.001$.

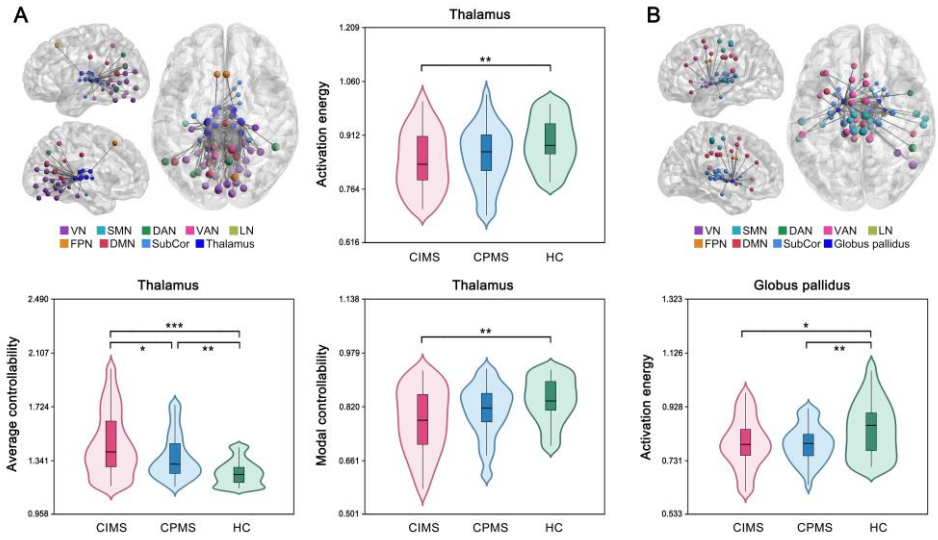

Figure 5. Controllability changes in the subcortical nuclei in CIMS and CPMS. (A) Both CIMS and CPMS showed increased average controllability in the thalamus when compared to HC, while CIMS further showed higher average controllability in the thalamus than CPMS; CIMS also exhibited decreased modal controllability and decreased activation energy in the thalamus compared to HC. (B) Both CIMS and CPMS showed decreased activation energy in the globus pallidus compared to HC. SubCor = subcortical network; $^{*}p < 0.050$; $^{**}p < 0.010$; $^{***}p < 0.001$.